**The EMBO Journal (2007) 26,** 3003–3014 | © 2007 European Molecular Biology Organization | All Rights Reserved 0261-4189/07
www.embojournal.org

THE EMBO JOURNAL

# Rice OsHKT2;1 transporter mediates large $Na^+$ influx component into $K^+$-starved roots for growth

**Tomoaki Horie[1], Alex Costa[1], Tae Houn Kim[1], Min Jung Han[2], Rie Horie[1], Ho-Yin Leung[1], Akio Miyao[3], Hirohiko Hirochika[3], Gynheung An[2] and Julian I Schroeder[1,*]**

[1]Division of Biological Sciences, Cell and Developmental Biology Section, and Center for Molecular Genetics, University of California, San Diego, La Jolla, CA, USA, [2]National Research Laboratory of Plant Functional Genomics, Department of Life Science, Pohang University of Science and Technology, Kyungbuk, Republic of Korea and [3]Division of Genome and Biodiversity Research, National Institute of Agrobiological Sciences, Ibaraki, Japan

**Excessive accumulation of sodium in plants causes toxicity. No mutation that greatly diminishes sodium ($Na^+$) influx into plant roots has been isolated. The OsHKT2;1 (previously named OsHKT1) transporter from rice functions as a relatively $Na^+$-selective transporter in heterologous expression systems, but the *in vivo* function of OsHKT2;1 remains unknown. Here, we analyzed transposon-insertion rice lines disrupted in *OsHKT2;1*. Interestingly, three independent *oshkt2;1*-null alleles exhibited significantly reduced growth compared with wild-type plants under low $Na^+$ and $K^+$ starvation conditions. The mutant alleles accumulated less $Na^+$, but not less $K^+$, in roots and shoots. *OsHKT2;1* was mainly expressed in the cortex and endodermis of roots. $^{22}Na^+$ tracer influx experiments revealed that $Na^+$ influx into *oshkt2;1*-null roots was dramatically reduced compared with wild-type plants. A rapid repression of OsHKT2;1-mediated $Na^+$ influx and mRNA reduction were found when wild-type plants were exposed to 30 mM NaCl. These analyses demonstrate that $Na^+$ can enhance growth of rice under $K^+$ starvation conditions, and that OsHKT2;1 is the central transporter for nutritional $Na^+$ uptake into $K^+$-starved rice roots.**

*The EMBO Journal* (2007) **26,** 3003–3014. doi:10.1038/sj.emboj.7601732; Published online 31 May 2007
*Subject Categories*: membranes & transport; plant biology
*Keywords*: HKT; $Na^+$ uptake; salt stress

## Introduction

Sodium ($Na^+$) is an alkali cation, which is not accumulated at large concentrations in most plant cells, in contrast to the alkali cation potassium ($K^+$), which is an essential macronutrient for plant growth. High concentrations of external $Na^+$ inhibit $K^+$ absorption (Rains and Epstein, 1965, 1967b) and elevated $Na^+$ concentrations in plant cells disturb functions of vital enzymes (Murguía *et al*, 1995) and photosynthesis (Tsugane *et al*, 1999), leading to $Na^+$ toxicity and cell death. On the other hand, classical plant physiological studies have reported a positive effect of low $Na^+$ concentrations on the growth of many plant species, but the underlying $Na^+$ uptake mechanisms remain unknown (Flowers and Läuchli, 1983).

Several genes that encode $Na^+$ permeable transporters/channels have been identified in plants. Biochemical analyses of vacuoles revealed a mechanism for the sequestration of $Na^+$ into vacuoles under salt stress via $Na^+/H^+$ antiporters (Blumwald and Poole, 1985, 1987). Genome sequencing of *Arabidopsis thaliana* led to the identification of the corresponding plant $Na^+/H^+$ antiporter genes, *AtNHX1* to *6* (Apse *et al*, 1999; Gaxiola *et al*, 1999; Yokoi *et al*, 2002; Aharon *et al*, 2003). An essential salt tolerance gene of *Arabidopsis*, salt overly sensitive 1 (*SOS1*), also belongs to the same $H^+$ exchanger family of transporters (Shi *et al*, 2000). The SOS1 transporter has been reported to function in long-distance $Na^+$ transport from roots to shoots in xylem parenchyma cells during salt stress (Shi *et al*, 2002).

Electrophysiological analyses using root cortex cells and suspension cultured cells of monocot plants suggest that toxic $Na^+$ influx into roots under high external $Na^+$ concentrations is mediated by voltage-independent channels (VIC) or non-selective cation channels (NSC) (Amtmann *et al*, 1997; Roberts and Tester, 1997; Tyerman *et al*, 1997; Buschmann *et al*, 2000; Davenport and Tester, 2000). VIC/NSC currents have also been reported in *Arabidopsis* roots and were shown to be downregulated by addition of cAMP and cGMP (Maathuis and Sanders, 2001). Recently, the cyclic nucleotide-gated channel 3 (*CNGC3*) gene was proposed to mediate non-selective cation uptake in the root of *Arabidopsis* plants (Gobert *et al*, 2006). The detailed molecular identities of VIC/NSC, however, remain unknown and no genetic mutations have been isolated in any plant species, to date, that show a strong reduction in $Na^+$ influx into roots.

HKT-type transporters have been characterized in several plant and bacterial species (Schachtman and Schroeder, 1994; Rubio *et al*, 1995; Fairbairn *et al*, 2000; Uozumi *et al*, 2000; Horie *et al*, 2001; Golldack *et al*, 2002; Garciadeblás *et al*, 2003; Su *et al*, 2003; Ren *et al*, 2005; Tholema *et al*, 2005). TaHKT2;1 (previously named TaHKT1) (Platten *et al*, 2006), from wheat, has been shown to mediate at least two transport modes in heterologous expression systems, $K^+$–$Na^+$ co-uptake and $Na^+$ influx at high $Na^+$ concentrations (Rubio *et al*, 1995; Gassmann *et al*, 1996). Analyses of the ion transport specificity of AtHKT1;1, previously named AtHKT1, in *Arabidopsis* and OsHKT2;1 (OsHKT1) in rice revealed that these HKT1 transporters/channels showed a relatively $Na^+$-

*Corresponding author. Division of Biological Sciences, Cell and Developmental Biology Section, and Center for Molecular Genetics, Room 5214, University of California, San Diego, 9500 Gilman Drive, La Jolla, CA 92093-0116, USA. Tel.: +1 858 534 7759; Fax: +1 858 534 7108; E-mail: julian@biomail.ucsd.edu

**Received: 12 December 2006; accepted: 2 May 2007; published online: 31 May 2007**

selective transport activity relative to $K^+$ transport activity in yeast and *Xenopus* oocytes (Uozumi *et al*, 2000; Horie *et al*, 2001; Garciadeblás *et al*, 2003). Null mutations in *AtHKT1;1* (Mäser *et al*, 2002a; Gong *et al*, 2004) and a reduced-function mutant allele of *AtHKT1;1* (Berthomieu *et al*, 2003) cause $Na^+$ over-accumulation in shoots, resulting in leaf chlorosis. Detailed $^{22}Na^+$ influx studies showed that AtHKT1;1 does not mediate $Na^+$ influx into *Arabidopsis* roots (Berthomieu *et al*, 2003; Essah *et al*, 2003). Recent studies have shown that AtHKT1;1 in *Arabidopsis* and its closest homologue, SKC1 or OsHKT1;5 in rice, function by removing $Na^+$ from the xylem sap, thus reducing $Na^+$ accumulation in leaves (Ren *et al*, 2005; Sunarpi *et al*, 2005; Horie *et al*, 2006). Unlike *AtHKT1;1*, which is a single-copy gene in *Arabidopsis thaliana*, seven full-length *OsHKT* genes were identified in the japonica rice genome based on the completed genome sequence (Garciadeblás *et al*, 2003).

Molecular genetic identification of transporters that mediate $Na^+$ influx into plant roots is crucial for developing models of $Na^+$ uptake mechanisms into plant roots. In this study, we have isolated and characterized *OsHKT2;1*-disrupted rice plants from a *Tos17*-tagged population (Hirochika, 1997, 2001; Yamazaki *et al*, 2001), to determine the physiological role of the OsHKT2;1 transporter in rice. Here, we demonstrate that *oshkt2;1* loss-of-function mutant alleles cause a dramatic reduction in $Na^+$ influx into $K^+$-starved rice roots. We further demonstrate that OsHKT2;1 plays an exclusive role in nutritional $Na^+$ uptake into $K^+$-starved rice roots, with an apparent $Na^+$ affinity ($K_m$) of $\approx$280 to 330 μM. Interestingly, OsHKT2;1-mediated $Na^+$ influx does not cause $Na^+$ toxicity, owing to a rapid down-regulation of the OsHKT2;1 transporter upon $Na^+$ stress.

## Results

### *Isolation of oshkt2;1 mutants and corresponding TosWT plants*

Ion selectivity analyses of OsHKT2;1 expressed in yeast and *Xenopus* oocytes showed that OsHKT2;1 functions as a $Na^+$ transporter in these heterologous expression systems (Horie *et al*, 2001; Mäser *et al*, 2002b; Garciadeblás *et al*, 2003). But the *in vivo* function of OsHKT2;1 in rice remains unknown. We searched the rice *Tos17* insertion mutant database (Hirochika, 1997, 2001; Miyao *et al*, 2003) for a putative *OsHKT2;1* gene-disrupted line to be used for uncovering the physiological role of OsHKT2;1 in rice plants. The retrotransposon *Tos17* undergoes local transposition events only during tissue culture, but is stable and non-motile in rice plants. We identified five putative *OsHKT2;1* insertion alleles. Among them, three *oshkt2;1* alleles, named *oshkt2;1-1*, *oshkt2;1-2* and *oshkt2;1-3* (Figure 1A), were chosen for further characterization, based on the fertility of plants and the germination rate of seeds of the next generation. In addition, we pursued isolation of related *OsHKT2;1* wild-type (WT) control plants, named 'TosWT'. Each *Tos17* mutant line comprises an average of 8–10 insertions, which demands additional WT controls for characterization of mutants. TosWT control lines were isolated from the same seed populations as *oshkt2;1-1*, *oshkt2;1-2* and *oshkt2;1-3* by screening for individuals that show no insertion in the *OsHKT2;1* gene. Southern hybridization showed polymorphisms in autoradiographs, confirming the insertion in *OsHKT2;1* in each line

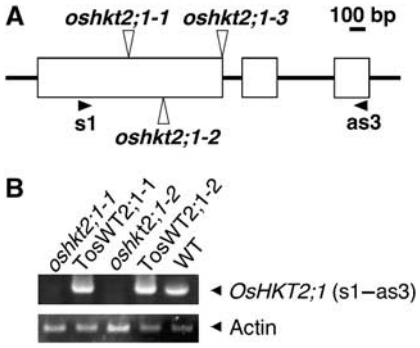


**Figure 1** Isolation of homozygous *Tos17* insertion mutants in the *OsHKT2;1* gene. (**A**) A schematic diagram of *oshkt2;1-1*, *oshkt2;1-2* and *oshkt2;1-3* alleles. White boxes represent exons. *oshkt2;1-3* has an insertion at the exon–intron boundary. s1 and as3 are primers used for RT–PCR. (**B**) RT–PCR analyses using cDNA derived from whole plant tissues of *oshkt2;1* mutant and WT plants (10-day old plants), which were grown under $K^+$ starvation conditions.

(data not shown). RT–PCR analyses using the primer set shown in Figure 1A showed that mature *OsHKT2;1* mRNA is missing in *oshkt2;1-1*, *oshkt2;1-2* plants (Figure 1B) and *oshkt2;1-3* (Supplementary Figure 1A). These data show the disruption of the *OsHKT2;1* gene in the *oshkt2;1-1*, *oshkt2;1-2* and *oshkt2;1-3* mutant lines.

### *oshkt2;1 mutant plants exhibit reduced growth under low $Na^+$ and $K^+$-starved conditions*

*oshkt2;1* and TosWT plants showed normal growth and were indistinguishable from WT cv. Nipponbare plants, either on soil or on ordinary nutrient media (Figure 2A and data not shown). A low-affinity $Na^+$ uptake mode of OsHKT2;1 has been hypothesized based on functional analyses, using heterologous expression systems (Horie *et al*, 2001). We thus first imposed NaCl stress (50–200 mM) on both soil grown and hydroponically grown plants. However, no notable difference in the visual phenotypes was observed between *oshkt2;1* and WT plants (data not shown).

The accumulation of *OsHKT2;1* mRNA was reported to dramatically increase in response to $K^+$ starvation (Horie *et al*, 2001; Garciadeblás *et al*, 2003). Ten-day old *oshkt2;1* plants grown in a 1 mM $CaSO_4$ ($K^+$ deprived) solution showed no visible growth defects and no differences in the fresh weight compared with TosWT plants (Figure 2B, $P>0.36$ for TosWT2;1-1 versus *oshkt2;1-1*; $P>0.08$ for TosWT2;1-2 versus *oshkt2;1-2*; Supplementary Figure 2A, $P>0.22$ for TosWT2;1-3 versus *oshkt2;1-3*). The plants were subsequently grown for 15 additional days in hydroponic culture medium containing 0.5 mM $NaNO_3$ (see Materials and methods). Fifteen days later, *oshkt2;1-1*, *oshkt2;1-2* and *oshkt2;1-3* mutant plants showed remarkably reduced growth, accompanied with a withering of the oldest leaf compared with TosWT2;1-1, TosWT2;1-2, TosWT2;1-3 and WT plants (Figure 2C and D and Supplementary Figure 2B and C). Fresh weights of *oshkt2;1* mutant plants were reduced approximately by 30–40% compared with TosWT plants (Figure 2E, $P<1.6\times10^{-5}$ for TosWT2;1-1 versus *oshkt2;1-1*; $P<7.1\times10^{-7}$ for TosWT2;1-2 versus *oshkt2;1-2*; Supplementary Figure 2D, $P<5.7\times10^{-6}$ for TosWT2;1-3 versus *oshkt2;1-3*). These data show that the OsHKT2;1 transporter

 

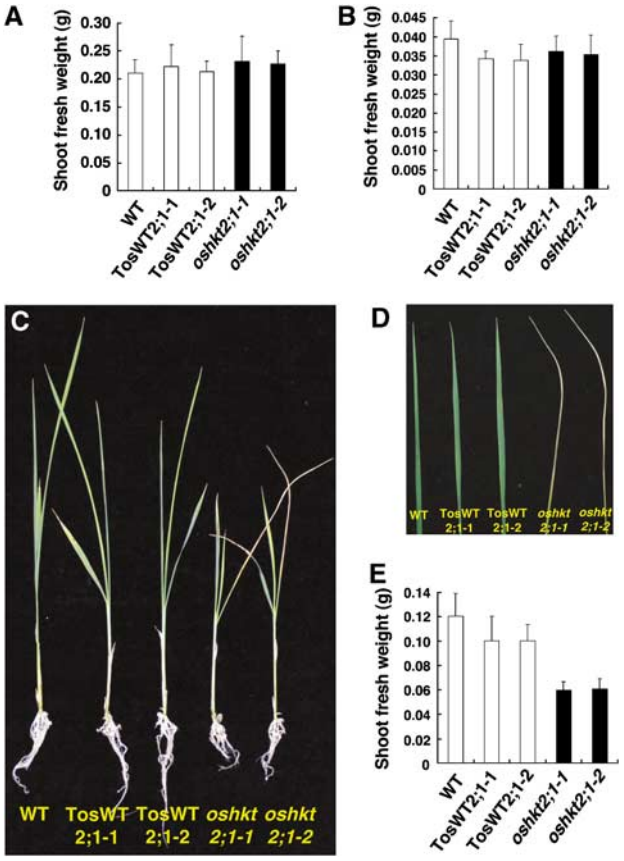


**Figure 2** *oshkt2;1* mutant plants show reduced growth under low $Na^+$ and $K^+$-starved growth conditions. (**A**) Fresh weights of 25-day-old WT, TosWT2;1-1, TosWT2;1-2, *oshkt2;1-1* and *oshkt2;1-2* plants, which were grown under 1.25 mM $K^+$ conditions for the last 15 days ($n=12$; $\pm$s.d.). (**B**) Fresh weights of WT, TosWT2;1-1, TosWT2;1-2, *oshkt2;1-1* and *oshkt2;1-2* plants, which were germinated and grown in 1 mM $CaSO_4$ solution for 10 days ($n=18$; $\pm$s.d.). (**C, D**) Twenty-five-day-old plants, which were grown under hydroponic conditions for the last 15 days in the presence of 0.5 mM $Na^+$ in a $K^+$-free medium. *oshkt2;1* mutant plants showed reduced growth (C) and chlorotic withering of the oldest leaves (D). Representative photographs of plants are shown and were observed in three independent experiments with over 18 total plants of each line. (**E**) Fresh weights of 25 day-old WT, TosWT2;1-1, TosWT2;1-2, *oshkt2;1-1* and *oshkt2;1-2* plants, which were grown under the same 0.5 mM $Na^+$ condition for the last 15 days as in (C) and (D) ($n=12$; $\pm$s.d.).

allows improved growth of WT plants under low nutrient $K^+$-starved conditions when 0.5 mM $NaNO_3$ was added to the growth solution.

### *oshkt2;1 mutant plants accumulate less $Na^+$ in both shoots and roots*

We determined $Na^+$ contents of *oshkt2;1* mutant, TosWT and WT plants. Ten-day-old plants grown in 1 mM $CaSO_4$ solution were transferred onto minimal medium containing 0.5 mM $Na^+$ and grown for nine additional days. Interestingly, *oshkt2;1-1*, *oshkt2;1-2* and *oshkt2;1-3* mutant plants were found to accumulate considerably less $Na^+$ in both roots and shoots compared with TosWT and WT plants (Figure 3 and Supplementary Figure 3). These results show that OsHKT2;1 functions in $Na^+$ accumulation in roots and also in shoots.

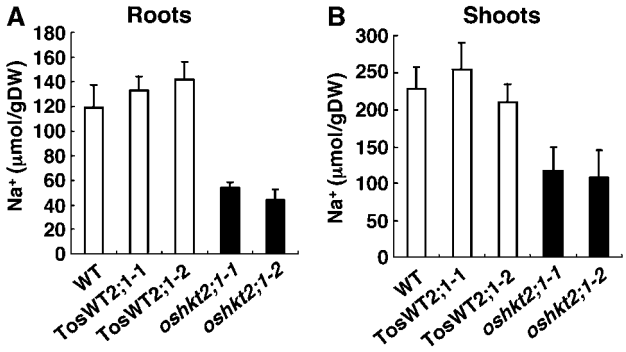


**Figure 3** *oshkt2;1* mutant plants accumulate less $Na^+$ in roots and shoots. Nineteen-day-old plants, which were hydroponically cultured under 0.5 mM $Na^+$- and $K^+$-free conditions for the last 9 days, were used. $Na^+$ contents of roots (**A**) and shoots (**B**) were measured by ICP-OES. Error bars represent standard deviations ($n=6$).

### *OsHKT2;1 expression in cortical and endodermal cells in roots and in vascular bundle regions in leaves*

Transgenic rice plants carrying the 1.6 kb *OsHKT2;1* promoter-β-glucuronidase (GUS) or green fluorescence protein (GFP) gene constructs were produced in order to determine the expression pattern of *OsHKT2;1*. Strong GUS signals were found in the main root but not in the root tip region (Figure 4A and B). Sections of GUS-stained roots further showed that cortex cells and endodermis cells were strongly stained (Figure 4C, see red stain). Sections of GUS-stained leaves showed the expression of *OsHKT2;1* in vascular bundle regions (Figure 4D and E).

Tissue expression of *OsHKT2;1* was further analyzed using transgenic plants expressing *GFP* driven by the 1.6 kb *OsHKT2;1* promoter. Roots of hygromycin B-resistant plants were briefly stained with propidium iodide (Swarup *et al*, 2004). Fluorescence was analyzed by confocal microscopy. A strong GFP fluorescence was found in root cortex cells of $K^+$-starved main roots (Figure 4 F, H and I). The tissue specificity of *OsHKT2:1* expression in $K^+$-starved roots of japonica rice presented in this study overlaps with, but also slightly differs from the expression pattern in indica rice varieties (Golldack *et al*, 2002). The reason for this discrepancy could be the difference in the regulation of *OsHKT2;1* expression between the two rice varieties and experimental conditions.

To analyze the transcriptional regulation of *OsHKT2;1* in response to external $K^+$ and $Na^+$ concentrations, *OsHKT2;1* promoter-*GFP* plants were grown in 1 mM $CaSO_4$ solution supplemented with either 30 mM $K^+$ or 30 mM $Na^+$. Addition of 30 mM $K^+$ or 30 mM $Na^+$ led to substantial reductions in GFP fluorescence of root cells (Figure 4J and K) compared with those of $K^+$-starved roots (Figure 4H). GFP and propidium iodide fluorescence intensities were quantified based on 3D reconstruction images obtained by z-series stacking and GFP fluorescence intensities and normalized to propidium iodide fluorescence intensities. The average GFP fluorescence intensity of $K^+$-starved roots was approximately five times higher than that of 30 mM $K^+$- or 30 mM $Na^+$-treated roots (Figure 4L). Taken together, these results demonstrate that the *OsHKT2;1* gene is mainly expressed at the cortex cell layer and the endodermal cell layer of $K^+$-starved japonica rice roots, and that *OsHKT2;1* gene expres-

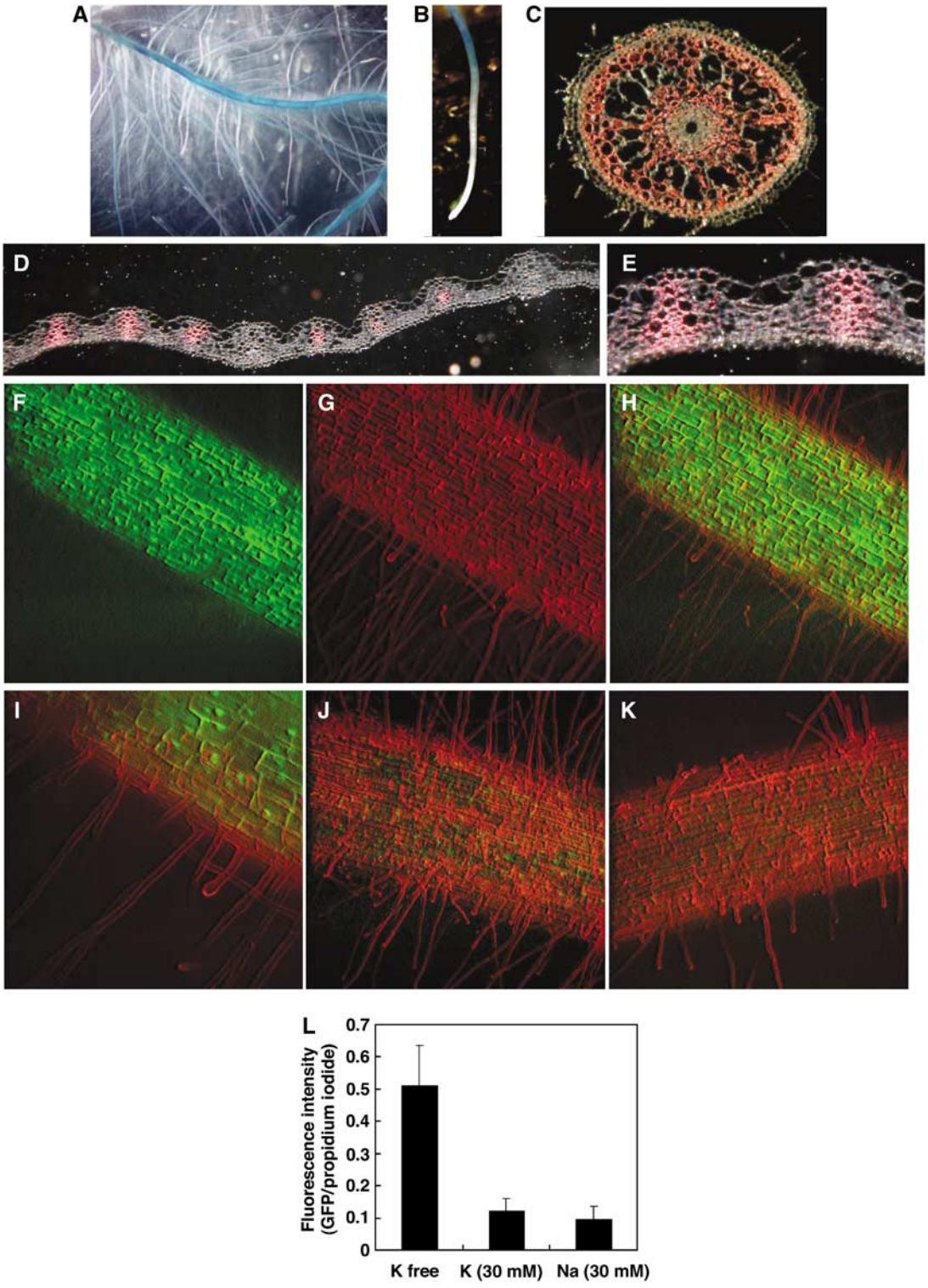


**Figure 4** *OsHKT2;1* gene expression in the cortex and endodermis of $K^+$-starved roots and in leaf vascular bundles. Transgenic rice plants expressing GUS or GFP reporter genes under the control of a 1.6 kb *OsHKT2;1* promoter were grown in 1 mM $CaSO_4$ solution in the presence of hygromycin. (**A, B**) Strong GUS staining was detected in main roots (A) but not in root tip regions (B). (**C**) A dark-field microscopic image of sections derived from GUS-stained main roots. Sections of GUS-stained (red staining) main roots showed strong signals in cortical and endodermal cells. (**D, E**) Dark-field microscopic images of sections derived from GUS-stained leaves. The sections showed strong GUS signals (red stain) in vascular bundle regions. In (E) is an enlarged image of a section of the region shown in (D). Note that the reddish staining in (C–E) shows GUS signals, as these were obtained using dark-field microscopy. (**F**) A 3D reconstruction image of GFP fluorescence derived from $K^+$-starved roots of *OsHKT2;1* promoter-GFP plants, showing strong GFP fluorescence in root cortex cells. (**G**) A 3D reconstruction image of propidium iodide fluorescence derived from $K^+$-starved roots of the same plant shown in (F). (**H**) Combined images of GFP and propidium iodide fluorescence shown in (F) and (G). (**I**) An enlarged image of $K^+$-starved roots shown in (H). (**J, K**) Combined images of GFP and propidium iodide fluorescence derived from 10-day-old *OsHKT2;1* promoter-GFP plants grown in 1 mM $CaSO_4$ solution supplemented with either 30 mM $K^+$ (J) or 30 mM $Na^+$ (K). (**L**) GFP fluorescence from three different conditions were quantified and normalized relative to propidium iodide fluorescence. Fluorescence intensities of GFP and propidium iodide in (J) were measured using three independent plants for each ionic condition ($\pm$s.d.).

sion is controlled by external $K^+$ and $Na^+$ concentrations at the transcriptional level.

### *oshkt2;1 mutant plants accumulate less $Na^+$ in the xylem sap*

We next determined $Na^+$ contents of the xylem sap. Ten-day-old *oshkt2;1* mutant and TosWT plants grown in 1 mM $Ca^{2+}$ solution were transferred to hydroponic nutrient medium containing 0.5 mM $Na^+$ and cultured for 2 days. Xylem sap was collected and $Na^+$ concentrations were determined by inductively coupled plasma-optic emission spectroscopy (ICP-OES). The results clearly showed that *oshkt2;1-1* and *oshkt2;1-2* mutant plants contained much less $Na^+$ compared with TosWT plants (Figure 5). $Na^+$ levels in the xylem sap of *oshkt2;1-1* were reduced by approximately 81.0% compared with TosWT2;1-1 (Figure 5A, $P<0.0008$ for *oshkt2;1-1* versus TosWT2;1-1) and those of *oshkt2;1-2* were reduced by approximately 89% compared with TosWT2;1-2 (Figure 5B, $P<0.001$ for *oshkt2;1-2* versus TosWT2;1-2).

### *OsHKT2;1 localization at the plasma membrane*

To gain insight into the subcellular localization of the OsHKT2;1 protein in plant cells, a chimeric *EGFP-OsHKT2;1* cDNA was constructed and placed downstream of the CaMV 35S promoter. Transient expression analyses were performed using tobacco leaf mesophyll cells. A bright fluorescence bordering the cell was found in mesophyll cells expressing EGFP-OsHKT2;1 (Figure 6A). Cells were subsequently stained with the plasma membrane marker FM4-64 (Bolte *et al*, 2004). As shown in Figure 6B, FM4-64-derived red fluorescence was detected at the border of cells. Combined images showed an overlap of the two different fluorescence emissions at the border of cells (Figure 6C and E), indicating that the EGFP-OsHKT2;1 protein localizes at the plasma membrane. Fluorescence images derived from EGFP and FM4-64 were analyzed in control experiments. In controls, green fluorescence was more broadly observed in the cell, including in the nucleus (Figure 6D), compared with EGFP-OsHKT2;1-derived fluorescence (Figure 6A). Native red chloroplast fluorescence showed the localization of chloroplasts, in addition to the plasma membrane staining with FM4-64 (Figure 6D). Combined images showed that EGFP-derived fluorescence and FM4-64-derived fluorescence did not overlap at the plasma membrane (Figure 6D and F), indicating that the EGFP control protein does not localize at the plasma membrane.

Subcellular localization of EGFP-OsHKT2;1 was also tested using *Arabidopsis* leaf epidermal cells. An EGFP-OsHKT2;1 and a control construct were introduced into epidermal cells by particle bombardment. Epidermal cells expressing the EGFP-OsHKT2;1 construct showed fluorescence at the border of cells (Figure 6G). In contrast, cells harboring a control

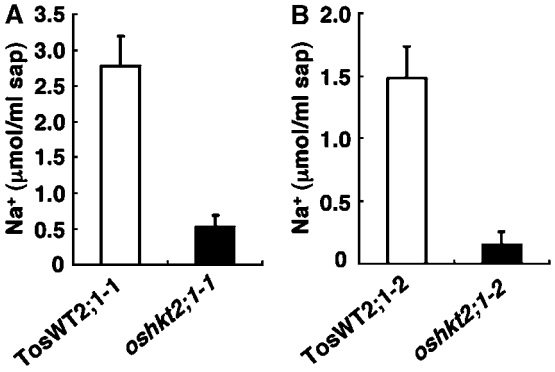


**Figure 5** *oshkt2;1* mutant plants accumulate less $Na^+$ in the xylem sap. Ten-day-old seedlings grown in 1 mM $CaSO_4$ solution were subsequently grown in 0.5 mM $Na^+$- and $K^+$-free conditions two more days. Xylem sap was collected from WT, TosWT2;1-1, TosWT2;1-2, *oshkt2;1-1* and *oshkt2;1-2*. $Na^+$ contents were measured by ICP-OES. (**A**) TosWT2;1-1 versus *oshkt2;1–1*. (**B**) TosWT2;1-1 versus *oshkt2;1-1*. Xylem sap extractions for (A) were performed at a different time of year than (B). Error bars represent standard error ($n=8$).

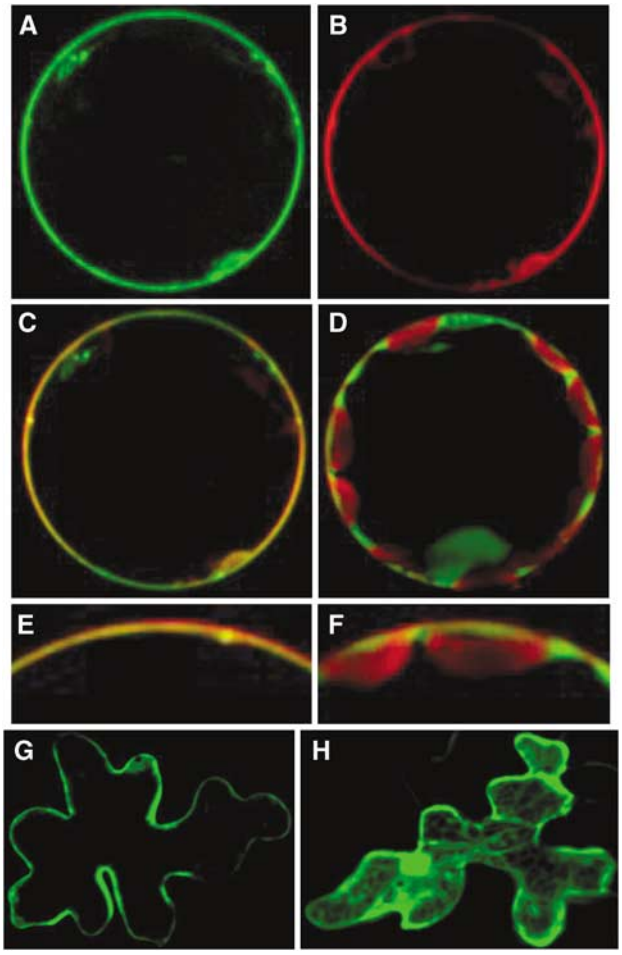


**Figure 6** OsHKT2;1 localizes at the plasma membrane of plant cells. EGFP-*OsHKT2;1* cDNA and EGFP were transiently expressed in protoplasts of tobacco mesophyll cells (**A–F**) and *Arabidopsis* epidermal cells (**G, H**) under the control of the 35S promoter. Fluorescence was analyzed by confocal microscopy. (A) GFP fluorescence of tobacco mesophyll cell protoplast expressing EGFP-*OsHKT2;1*. (B) FM4-64 plasma membrane marker fluorescence emitted from the same protoplast shown in (A). (C) Combined images of GFP and FM4-64 fluorescence shown in (A) and (B). (D) Combined images of GFP control and FM4-64 fluorescence, derived from cells harboring a control construct. Note that native red chloroplast autofluorescence was observed in addition to red FM4-64 fluorescence at the plasma membrane (D, F). (E) An enlarged image of (C). (F) An enlarged image of (D). (G) GFP fluorescence of *Arabidopsis* epidermal cells expressing EGFP-*OsHKT2;1*. (H) GFP fluorescence of *Arabidopsis* epidermal cells harboring a GFP control construct.

construct showed ubiquitous fluorescence in the cytoplasm and in the nucleus (Figure 6H). Taken together, these transient expression analyses provide evidence that the OsHKT2;1 transporter localizes at the plasma membrane of plant cells.

### *Severe disruption of $Na^+$ influx in oshkt2;1 mutant roots*

Less $Na^+$ accumulation in shoots and roots of *oshkt2;1* mutants (Figure 3) and localization analyses of OsHKT2;1 (Figures 4 and 6) indicated that OsHKT2;1 may mediate $Na^+$ influx into rice roots. In order to test this hypothesis, we performed short-term tracer influx experiments using $^{22}Na^+$. Time-dependent $Na^+$ influx into roots of intact rice plants was monitored at 0.1 mM external $Na^+$ using 10-day-old *oshkt2;1-1*, *oshkt2;1-2*, *oshkt2;1-3*, TosWT2;1-1, TosWT2;1-2, TosWT2;1-3 and WT plants, which were grown in 1 mM $CaSO_4$ solution. Interestingly, short-term $Na^+$ influx into rice roots at 0.1 mM external $Na^+$ was almost completely abolished in *oshkt2;1-1*, *oshkt2;1-2* and *oshkt2;1-3* plants, while TosWT2;1-1, TosWT2;1-2, TosWT2;1-3 and WT plants exhibited similar $Na^+$ influx time courses (Figure 7A and Supplementary Figure 4A).

Detailed concentration-dependent $Na^+$ influx studies were performed in the 'high-affinity' $Na^+$ uptake range, at 1, 5, 10, 25, 50, 100 and 200 μM external $Na^+$, using *oshkt2;1* mutant plants and TosWT plants. *oshkt2;1-1* and *oshkt2;1-2* plants showed severe $Na^+$ influx reductions compared with TosWT2;1-1 and TosWT2;1-2 plants (Figure 7B; 92.7% reduction at 200 μM). We further characterized $^{22}Na^+$ influx kinetics of *oshkt2;1* mutants and TosWT plants at higher external $Na^+$ concentrations of up to 5000 μM. Sodium influx into roots of *oshkt2;1-1* and *oshkt2;1-2* plants within this range was severely reduced compared with that of TosWT2;1-1 and TosWT2;1-2 (Figure 7C). Sodium influx in *oshkt2;1* mutant lines showed a reduction of $^{22}Na^+$ influx by approximately 88–90% of WT controls at 500 μM $Na^+$, 86–88% at 1000 μM $Na^+$ and 63–67% at 5000 μM $Na^+$, respectively.

Michaelis–Menten analyses were performed using concentration-dependent $Na^+$ influx data obtained at 1–5000 μM external $Na^+$. A single-uptake phase formalism described the

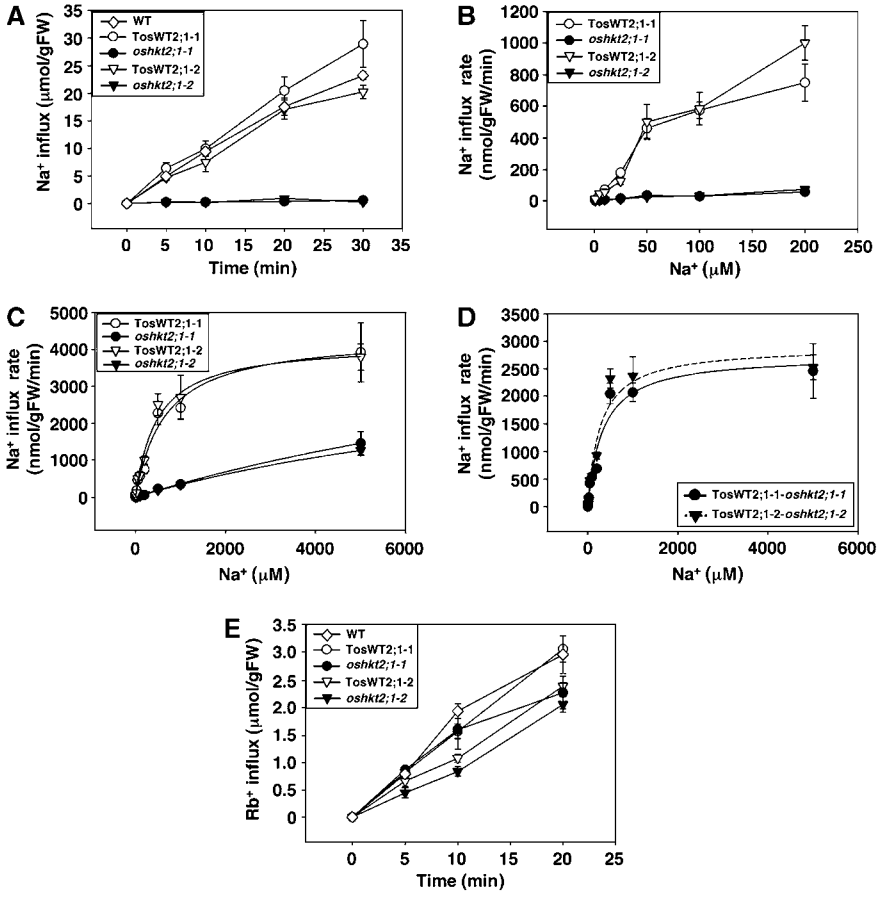


**Figure 7** Short-term $^{22}Na^+$ influx analyses show that OsHKT2;1 functions as a major $Na^+$ uptake pathway in $K^+$-starved rice roots. Plants were grown in 1 mM $CaSO_4$ solution for 10 days. Time-dependent and concentration-dependent $^{22}Na^+$ influx experiments were performed using $^{22}NaCl$ as a tracer. (**A**) Time-dependent $Na^+$ influx into roots of WT, TosWT2;1-1, TosWT2;1-2, *oshkt2;1-1* and *oshkt2;1-2* at 0.1 mM external $Na^+$ ($n=3$; ±s.d.). (**B**) Concentration-dependent $Na^+$ influx into roots of TosWT2;1-1, TosWT2;1-2, *oshkt2;1-1* and *oshkt2;1-2* at 1, 5, 10, 25, 50, 100 and 200 μM external $Na^+$ ($n=3$; ±s.d.). (**C**) Concentration-dependent $Na^+$ influx into roots of TosWT2;1-1, TosWT2;1-2, *oshkt2;1-1* and *oshkt2;1-2* at 1–5000 μM external $Na^+$ ($n=3$; ±s.d.). Curves in (C) are plotted separately for each WT and *oshkt2;1* mutant allele derived from Michaelis–Menten analyses of the data (Table Ia). (**D**) OsHKT2;1-dependent $Na^+$ influx rates of rice roots. Differences in $Na^+$ influx rates between TosWT and *oshkt2;1* mutant plants are shown (±s.d.). Curves in (D) were derived from Michaelis–Menten analyses (Table Ib). (**E**) Time-dependent $Rb^+$ ($K^+$) influx into roots of WT, TosWT2;1-1, TosWT2;1-2, *oshkt2;1-1* and *oshkt2;1-2* at 0.1 mM external $Rb^+$ ($n=6$; ±s.d.).

**Table I** Michaelis–Menten curve-fitting results for $^{22}Na^+$ influx kinetics in intact rice roots of $K^+$-starved oshkt2;1 mutant and TosWT2;l control plants (Figure 7C), and for OsHKT2; 1-dependent $Na^+$ uptake rates in rice roots (Figure 7D)

| | | $R^2$ | $K_M$ (μM) | $V_{max}$ (nmol/gFW/min) |
|---|---|---|---|---|
| a | TosWT2;1-l | 0.981 | 655.52 ± 114.17 | 4390.10 ± 272.26 |
| | TosWT2;1-2 | 0.985 | 477.82 ± 74.45 | 4176.83 ± 219.04 |
| | *oshkt2;1-1* | 0.998 | 15 764.47 ± 3639.95 | 6051.83 ± 1082.91 |
| | *oshkt2;1-2* | 0.999 | 11 499.50 ± 579.23 | 4165.29 ± 149.14 |
| b | TosWT2;1-1-*oshkt2;1-1* | 0.958 | 280.4 ± 74,8 | 2901.1 ± 236.6 |
| | TosWT2;1-2-*oshkt2;1-2* | 0.964 | 330.9 ± 81.6 | 2744.5 ± 213.2 |

Curve fitting was performed with SigmaPlot 8.0 (SPSS, Chicago) software. Results from a one-term Michaelis–Menten equation. Fitting results to the data derived from TosWT and *oshkt1* mutant plants are shown in (a) (see results and Figure 7C). (b) Fitting results to the values, which represent the difference in $Na^+$ influx rates between *oshkt2;1* mutant and TosWT2:l plants.

kinetics of $Na^+$ influx better in rice roots than a two-uptake phase analysis (Table Ia). The fitting results are plotted in Figure 7C for each WT and mutant allele. These results demonstrated that the disruption of the *OsHKT2;1* gene dramatically affected the affinity of rice roots for $Na^+$ and caused a severe $Na^+$ uptake reduction (average $K_m$ shift from 550 μM to 13.6 mM) (Table Ia). To approximate OsHKT2;1-dependent $Na^+$ influx into rice roots, $Na^+$ influx rates of *oshkt2;1* mutants were subtracted from the corresponding rates of TosWT plants. Michaelis–Menten analysis predicted an apparent affinity for the OsHKT2;1-dependent $Na^+$ influx into roots of ≈280 to 330 μM $Na^+$ and a $V_{max}$ of ≈2750 to 2900 nmol/gFW/min (Figure 7D; Table Ib). These flux analyses demonstrate that OsHKT2;1 mediates $Na^+$ influx into roots and composes a major component for $Na^+$ uptake into $K^+$-starved rice roots in a broad concentration range.

### *Intact $K^+$ ($Rb^+$) uptake in oshkt2;1 mutant plants*

To determine whether *OsHKT2;1* mutations have an influence on $K^+$ uptake in intact rice roots, tracer influx experiments using $^{86}Rb^+$ were performed. *oshkt2;1* mutant, TosWT and WT plants, grown in 1 mM $CaSO_4$ solution, were used for time-dependent $Rb^+$ influx assays at 100 μM external $Rb^+$. Only very small differences were detected between *oshkt2;1* mutants and the WT lines, which showed a linear increase in $Rb^+$ influx under the imposed condition (Figure 7E), in contrast to $Na^+$ influx (Figure 7A). These results show that mutations in the *OsHKT2;1* gene do not have a strong impact on high-affinity $K^+$ ($Rb^+$) uptake into intact rice roots. Small differences may be due to indirect effects of the *oshkt2;1* mutations (e.g. on membrane potential).

### *Toxic sodium levels rapidly downregulate OsHKT2;1 transporter function in rice roots*

To determine whether OsHKT2;1-mediated $Na^+$ influx is affected by the amount of applied $K^+$ or $Na^+$ concentrations, *oshkt2;1* mutant, TosWT and WT plants were grown in 1 mM $CaSO_4$ solution including either 5 mM KCl or 30 mM NaCl. $^{22}Na^+$ influx was monitored at 0.1 mM external $Na^+$ (Figure 8A and Supplementary Figure 4B) and 1.0 mM external $Na^+$ (Figure 8B and Supplementary Figure 4C). Interestingly, when the growth medium was supplemented with either 5 mM $K^+$ or 30 mM $Na^+$, $Na^+$ influx into roots of TosWT and WT plants was dramatically repressed (Figure 8A and B). Comparisons with $^{22}Na^+$ influx rates of *oshkt2;1* knockout mutant plants demonstrated that the *OsHKT2;1*-mediated $Na^+$ influx is tightly regulated by the level of external $K^+$ and $Na^+$ in the growth medium (Figure 8A, and B).

The time course of $Na^+$ influx repression was further analyzed. Sodium influx in WT plants at 0.1 mM $Na^+$ was monitored at six time points after the addition of 30 mM NaCl into the 1 mM $CaSO_4$ growth solution. The $^{22}Na^+$ influx time course demonstrated that OsHKT2;1-dependent $Na^+$ influx is rapidly repressed in response to addition of 30 mM NaCl (Figure 8C; half time = 1.45 ± 0.11 h).

Several inhibitors were applied to gain initial insight into the biological mechanism(s) that mediates the rapid repression of the OsHKT2;1 transporter upon $Na^+$ stress. A solution composed of *N*-methyl-D-glucamine (NMDG) was first tested as a source of a relatively membrane impermeable cation. The results showed that 30 mM NMDG solution was not effective at evoking the repression of the OsHKT2;1 compared with 30 mM $Na^+$ (Figure 8D, b). The transcriptional inhibitor actinomycin D (20 μg/ml), the translational inhibitor cycloheximide (100 μM), as well as the proteasome inhibitor MG132 (50 μM), all did not greatly affect the 30 mM NaCl-induced rapid repression (Figure 8D, d–f). On the other hand, the serine/threonine protein kinase inhibitor K252a caused a more severe repression of $Na^+$ influx than the effect of 30 mM NaCl (Figure 8D, g).

Quantitative real-time RT–PCR analyses of *OsHKT2;1* mRNA upon the addition of 30 mM NaCl were subsequently performed. Interestingly, time-course analyses showed that the addition of NaCl caused a rapid reduction of *OsHKT2;1* mRNA (Figure 8E; $n = 4$ replicates). These data suggest that both posttranslational (Figure 8D) and transcript expression (Figure 8E) mechanisms control OsHKT2;1 activity in intact rice roots.

## Discussion

Several *Arabidopsis* mutants such as *sos1* (Wu *et al*, 1996; Shi *et al*, 2002), *atnhx1* (Apse *et al*, 2003) and *athkt1;1* (Rus *et al*, 2001; Mäser *et al*, 2002a; Berthomieu *et al*, 2003), which are disrupted or mutated in genes encoding $Na^+$ transporters, have been characterized. These reports have demonstrated that the $Na^+$ transporters in *Arabidopsis*, SOS1, AtNHX1 and AtHKT1;1, function to protect *Arabidopsis* plants from salt stress by different mechanisms (Zhu, 2002; Horie and Schroeder, 2004). *HKT* cDNAs have been isolated and characterized from many plant species (Fairbairn *et al*, 2000; Uozumi *et al*, 2000; Horie *et al*, 2001; Golldack *et al*, 2002; Garciadeblás *et al*, 2003; Su *et al*, 2003; Ren *et al*, 2005).

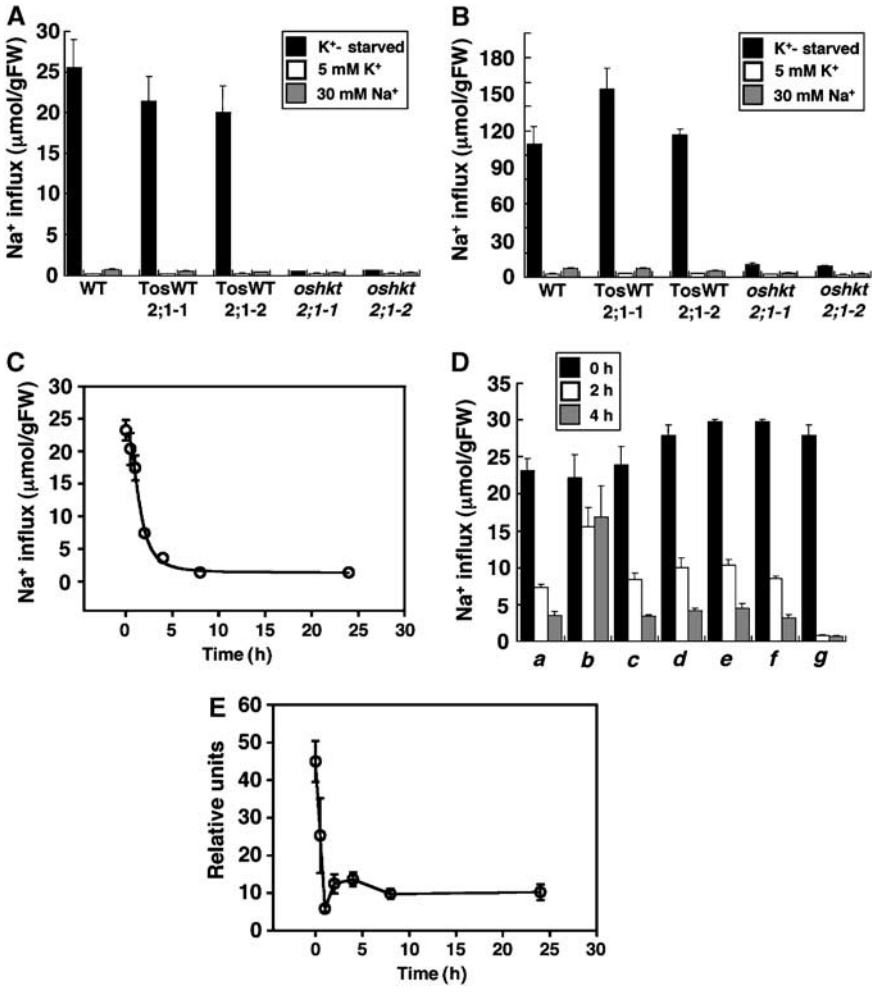


**Figure 8** Sodium influx into $K^+$-starved rice roots via OsHKT2;1 is subjected to posttranslational inactivation in response to high external $Na^+$. (**A, B**) Sodium influx into roots of 10-day-old WT, TosWT2;1-1, TosWT2;1-2, *oshkt2;1-1* and *oshkt2;1-2*, which were grown either in 1 mM $CaSO_4$ solution (black bars), or the same solution supplemented with 5 mM KCl (white bars), or the 1 mM $CaSO_4$ solution supplemented with 30 mM $Na^+$ (gray bars). Sodium influx into roots was monitored at 0.1 mM external $Na^+$ (A) and 1.0 mM external $Na^+$ concentrations (B) ($n=3$; ±s.d.) 20 min after exposure of roots to the indicated solutions. (**C**) Time-dependent repression of $Na^+$ influx into $K^+$-starved rice roots via OsHKT2;1 in response to addition of 30 mM NaCl ($n=3$; ±s.d.). (**D**) Repression of OsHKT2;1-mediated $Na^+$ influx in response to inhibitors. Sodium influx into roots of 10-day-old WT plants grown in 1 mM $CaSO_4$ solution (0 h black bars) or plants incubated with the indicated test solutions for 2 h (white bars), or plants incubated with test solutions for 4 h (gray bars) are shown. Solutions contained (a) 30 mM NaCl, (b) 30 mM *N*-methyl-D-glucamine–Cl, (c) 30 mM NaCl and 0.1% DMSO, (d) 30 mM NaCl and the proteasome inhibitor MG132 (50 μM), (e) 30 mM NaCl and actinomycin D (20 μg/ml), (f) 30 mM NaCl and the translational inhibitor cycloheximide (100 μM), and (g) 30 mM NaCl and 5 μM K252a. Time-dependent sodium influx into roots shown in (C, D) was monitored at 0.1 mM external $Na^+$ ($n=3$; ±s.d.). (**E**) Time-course expression analyses of the *OsHKT2;1* mRNA in roots in response to 30 mM NaCl by quantitative real-time RT–PCR. Expression levels of *OsHKT2;1* were monitored at 0, 0.5, 1, 2, 4, 8 and 24 h after the addition of 30 mM NaCl. The *OsHKT2;1* expression level of plants grown in 1 mM $CaSO_4$ solution supplemented with 30 mM KCl was also analyzed as a reference of basal *OsHKT2;1* expression. All data were normalized to the level of the constitutively expressed *OsSMT3* mRNA expression. *OsHKT2;1* mRNA levels are plotted relative to the basal *OsHKT2;1* expression level. Data at each time point show the average ± s.e. of four independent experiments.

*TaHKT2;1*-antisense wheat plants have been shown to exhibit an approximately 42% decrease in $^{22}Na^+$ uptake at a high 100 mM external NaCl concentration, but no substantial difference in $^{22}Na^+$ influx at 20 and 50 mM NaCl concentrations (Laurie *et al*, 2002). Despite these advances, no strong $Na^+$ influx genetic mutant line has been identified in plants, indicating overlapping redundancies in $Na^+$ transporters that mediate $Na^+$ influx into plants (Schroeder *et al*, 1994). The present findings reveal that OsHKT2;1 mediates a major contribution to $Na^+$ influx into $K^+$-starved roots. An approximately 10–30% $Na^+$ influx activity at millimolar concentrations remains in *oshkt2;1-1* and *oshkt2;1-2* mutant plants (Figures 7 and 8). Studies investigating whether the remaining $Na^+$ influx in intact rice roots depends on other OsHKT transporters and/or different $Na^+$ permeable channels/transporters will be an interesting subject for future inquiry. Genome analysis of rice cv. Nipponbare led to the identification of seven expressed *OsHKT* genes (Garciadeblás *et al*, 2003). OsHKT1;5 (OsHKT8 or SKC1) and its closest homologue in *Arabidopsis*, AtHKT1;1 (AtHKT1), have been shown to function in salt tolerance by reducing $Na^+$ levels in the xylem sap (Ren *et al*, 2005; Sunarpi *et al*, 2005; Horie *et al*, 2006). More recently from initial mapping experiments, the *TaHKT7* (*TaHKT1;4*) and *TaHKT8* (*TaHKT1;5*) genes in durum wheat, close homologues of *AtHKT1;1*, have also been hypothesized to play a protective role in maintaining viability of wheat leaves under saline conditions (Huang *et al*, 2006; Byrt *et al*, 2007).

 

### *Genetic evidence that $Na^+$ enhances growth of rice plants and a major role for OsHKT2;1 in nutritional $Na^+$ uptake*

Unlike $K^+$, which is an essential macronutrient and the most abundant cation in plant cells, $Na^+$ is not required as an essential nutrient by most higher plants, including glycophytes, despite the fact that the availability of $Na^+$ and $K^+$ is in general similar. On the other hand, however, classic plant physiological studies have shown that moderate amounts of $Na^+$ enhance the growth of many plant species (Mengel and Kirkby, 1982; Flowers and Läuchli, 1983). Nutritional effects of $Na^+$ have been found on the growth of beet and tomato plants (Woolley, 1957; Marschner, 1971; Besford, 1978). Despite these physiological observations, no genetic evidence for growth enhancement by $Na^+$ has been obtained and genes mediating this process have not been identified.

*oshkt2;1-1* and *oshkt2;1-2* mutant plants were indistinguishable from WT plants under $K^+$-rich nutrient conditions (Figure 2A and data not shown). Interestingly, however, *oshkt2;1-1*, *oshkt2;1-2* and *oshkt2;1-3* plants exhibited reduced growth, accompanied by leaf chlorosis under low $Na^+$ and $K^+$-limiting conditions (Figure 2C–E and Supplementary Figure 2B–D). These results, together with $Na^+$ transport, accumulation and OsHKT2;1 localization analyses, provide first genetic evidence that $Na^+$ enhances growth of rice plants under $K^+$-starved condition, and that the plasma membrane transporter/channel OsHKT2;1 plays a central role in acquiring and distributing $Na^+$ as a 'nutrient'. Potassium depletion strongly induces *OsHKT2;1* gene expression (Figure 4H) (Horie *et al*, 2001; Golldack *et al*, 2002; Garciadeblás *et al*, 2003) and OsHKT2;1-dependent $Na^+$ influx in roots (Figure 8A and B). However, $Na^+$ does not completely rescue rice plants from $K^+$ deficiency (Figure 2A and E). Presumably, $Na^+$ replaces only some of the roles of $K^+$, which functions in many processes, including osmotic adjustment, enzyme activation, cell expansion, maintenance of membrane potential, protein synthesis and photosynthetic activity. Possible main functions of $Na^+$ for cellular viability in $K^+$-starved plants may be maintenance of turgor pressure and cell expansion.

### *$K^+$ ($Rb^+$) uptake and the OsHKT2;1 transporter in $K^+$-starved rice roots*

A $Na^+$-selective has been detected in ion selectivity analyses of OsHKT2;1 expressed in heterologous expression systems (Horie *et al*, 2001; Mäser *et al*, 2002b; Garciadeblás *et al*, 2003), with an exception in which similar $K^+$ and $Na^+$ transport were observed (Golldack *et al*, 2002). To test whether dysfunctional mutations in the *OsHKT2;1* gene affect net $K^+$ influx *in planta*, we performed short-term $^{86}Rb^+$ tracer influx analyses and compared the results between *oshkt2;1* mutants and WT plants. Small reductions in $^{86}Rb^+$ influx were detected in $^{86}Rb^+$ influx assays performed at 0.1 mM external RbCl (Figure 7E). Two not mutually exclusive explanations may account for this difference. OsHKT2;1 may have a small permeability to $K^+$. Alternatively, disruption of the *OsHKT2;1* gene may affect other $K^+$ influx transporters, for instance, by causing less hyperpolarized membrane potential in the $Na^+$-free $Rb^+$ influx buffers used for $Rb^+$ influx assays. A slightly less hyperpolarized membrane potential in *oshkt2;1* plants would indirectly result in decreasing net $Rb^+$ ($K^+$) influx in *oshkt2;1* mutant roots compared to WT plants. The relatively small effect of *oshkt2;1* disruption on $Rb^+$ influx compared with $Na^+$ influx shows that OsHKT2;1 mainly transports $Na^+$ *in planta* under the imposed conditions.

### *Downregulation of OsHKT2;1 in response to high levels of sodium*

Sodium over-accumulation in plant cells triggers diverse toxicities by perturbing vital cellular processes and reduces plant viability (Glenn *et al*, 1999; Zhu, 2002; Ward *et al*, 2003). Sodium influx into barley roots has been found to show multiple kinetic components (Rains and Epstein, 1967a), and an increase in the concentration of either $K^+$ or $Ca^{2+}$ in 50 mM $Na^+$ solution led to reductions of low-affinity $Na^+$ influx into $K^+$-starved barley roots (Rains and Epstein, 1967b), and in a reduction in external $Na^+$ depletion at 100 μM external $Na^+$ (Haro *et al*, 2005). *OsHKT2;1*-expressing yeast cells showed $Na^+$ hypersensitivity even under relatively mild stress conditions and OsHKT2;1 expressed in *Xenopus* oocytes yielded large $Na^+$-selective inward currents at 100 mM external $Na^+$ concentration (Horie *et al*, 2001). Furthermore, we found in this study that OsHKT2;1 mediates $Na^+$ influx into rice roots, with substantial $V_{max}$ values of ≈2700 to 2900 nmol/gFW/min (Figures 7C and D, 8A; Table Ib). It cannot be excluded that a portion of the OsHKT2;1-dependent $Na^+$ influx into intact roots (Figures 7, 8A and B) may be mediated by other transporters that are influenced by OsHKT2;1 activity (Schroeder *et al*, 1994). On the other hand, *oshkt2;1* knockout would cause more hyperpolarized potentials in the presence of $Na^+$, which can drive more $Na^+$ influx via other transporters, and thus $^{22}Na^+$ influx analyses of *oshkt2;1* mutants may underestimate $Na^+$ influx transported by OsHKT2;1.

OsHKT2:1 has been suggested to mediate high-affinity $Na^+$ uptake in roots of rice plants (Garciadeblás *et al*, 2003). The determined $K_m$ values in this study differ to a degree from the $K_m$ (20 μM) values for OsHKT2;1 expressed in yeast (Garciadeblás *et al*, 2003). The reason for this difference may be several factors, including homologous versus heterologous expression of OsHKT2;1, different membrane potentials and possibly measurements of external $Na^+$ depletion in yeast (Garciadeblás *et al*, 2003) compared to $^{22}Na^+$ influx here.

At high $Na^+$ concentrations of more than 25 mM, an apoplastic $Na^+$ influx pathway contributes to $Na^+$ uptake into rice roots (Yeo *et al*, 1987). The present study shows a major contribution of OsHKT2;1 to $Na^+$ influx at a wide concentration range. The maximum $Na^+$ influx rates of low-affinity $Na^+$ uptake components in $K^+$-starved barley roots, determined in the presence of 0.5–50 mM NaCl, can be estimated to approximately 4–5 times smaller than the $V_{max}$ values of *OsHKT2;1*-dependent $Na^+$ influx (Rains and Epstein, 1967a) (Table Ib). Maximum *OsHKT2;1*-dependent $Na^+$ influx rates with 1 mM $Ca^{2+}$ in the influx buffer (Figure 7D) were approximately twice as high as the $Na^+$ influx rate of *Arabidopsis* roots exposed to 50 mM NaCl and mM $Ca^{2+}$ (Essah *et al*, 2003). These findings and comparisons show that OsHKT2;1 can mediate substantial $Na^+$ influx rates in intact plants and suggest that OsHKT2;1-mediated $Na^+$ influx would potentially cause $Na^+$ toxicity in $K^+$-starved rice plants. In contrast, however, *oshkt2;1-1*

and *oshkt2;1-2* plants did not show any difference in salt sensitivity when treated with several high concentrations of NaCl, even under $K^+$-starved conditions (data not shown).

To investigate whether OsHKT2;1 contributes to toxic $Na^+$ influx, we performed tracer influx experiments, adding high levels of $Na^+$ to $K^+$-starved roots. Interestingly, OsHKT2;1-dependent $Na^+$ influx was rapidly repressed upon the addition of 30 mM NaCl to $K^+$-starved roots (Figure 8C). *OsHKT2;1* mRNA was also found to undergo rapid reduction in response to the addition of NaCl (Figure 8E). Use of proteasome, transcriptional, translational and protein kinase inhibitors suggests that rapid downregulation of OsHKT2;1-dependent $Na^+$ influx might not be directly and solely mediated by ubiquitination-related protein degradation, (Figure 8D, d–g). The rapid downregulation process correlates with *OsHKT2;1* mRNA degradation (Figure 8C, D (g), E). However, it should be noted that a relatively large and measurable level of *OsHKT2;1* mRNA remains even after the OsHKT2;1-dependent $Na^+$ influx is almost completely shut down (Figure 8C and E), suggesting that mechanisms such as phosphorylation-dependent posttranslational modifications could be contributing to the downregulation of OsHKT2;1-dependent $Na^+$ influx (Figure 8D, g).

In summary, the present study reports the identification of genetic mutants, *oshkt2;1-1* and *oshkt2;1-2*, that strongly reduce $Na^+$ influx into plant roots. Moreover, our findings provide robust genetic evidence that a moderate amount of $Na^+$ enhances the growth of rice plants as a nutrient and the *OsHKT2;1* gene is responsible for a major portion of nutritional $Na^+$ uptake and distribution in $K^+$-starved rice plants. OsHKT2;1 functions in $Na^+$-selective influx relative to $K^+$ *in planta*. Our findings also reveal that OsHKT2;1-induced $Na^+$ influx is rapidly downregulated by posttranslational and transcriptional mechanisms, which monitor and restrict the amount of $Na^+$ influx via OsHKT2;1 to prevent $Na^+$ overaccumulation and thus $Na^+$ toxicity. A complete elucidation of the molecular mechanisms that mediate rapid inactivation of OsHKT2;1 under high $Na^+$ concentrations will be an important subject for understanding mechanisms controlling nutritional $Na^+$ uptake and salinity resistance.

## Materials and methods

### *Plant materials and growth conditions*

Rice seeds were sterilized as described previously (Horie *et al*, 2001). Sterilized seeds were then planted on a plastic screen (Caisson labs, Sugar City, ID, USA) that was subsequently placed in a sterilized vessel (Caisson labs, Sugar City, ID, USA) filled with 1 mM $CaSO_4$ solution or the same solution supplemented with KCl or NaCl. Seedlings were grown under light/dark cycles of 16/8 h and a temperature regime of 28/26°C. Hydroponic cultures were conducted using a modified basic nutrient medium (Mäser *et al*, 2002a) composed of 1.25 mM $KNO_3$, 0.5 mM $NH_4H_2PO_4$, 0.5 mM $MgSO_4$, 0.5 mM $Ca(NO_3)_2$, 50 μM $Fe_2(SO_4)_3$, 26 μM $H_3BO_3$, 5 μM $ZnSO_4$ and 40 μM $MnSO_4$. For 0.5 mM $Na^+$-containing medium, $KNO_3$ was substituted with $NaNO_3$ and NMDG neutralized with $HNO_3$. pH was brought to 5.5 by NMDG. Seedlings grown in 1 mM $CaSO_4$ solution were transferred onto each modified medium using plugs (Jaece Industries Inc., North Tonawanda, NY, USA). Solutions were changed every 3 days.

Tobacco (*Nicotiana tabacum* cv. SR1) seeds were surface sterilized and sown on one-half Murashige and Skoog agar medium (Murashige and Skoog, 1962) containing 15 g/l sucrose. Tobacco plants were grown at 25°C and maintained by *in vitro* sterile shoot culture under light/dark cycles of 16/8 h in a growth chamber. *Arabidopsis* (*A. thaliana* ecotype Columbia) plants were grown on sterile soil for 20 days at 22°C under light/dark cycles of 16/8 h in a growth chamber.

### *Nucleic acid analyses and transgenic plants*

Standard methods for nucleic acid isolations and analyses, for reporter genes analyses and for plant transformations are given in Supplementary data.

### *Ion content determinations*

Ten-day-old plants grown in 1 mM $CaSO_4$ solution were transferred onto 0.5 mM $Na^+$-containing basic nutrient medium and hydroponically grown 9 further days. Ion contents of shoots and roots were measured by ICP-OES.

Ten-day-old plants grown in 1 mM $CaSO_4$ solution were exposed to 0.5 mM $Na^+$-containing basic nutrient medium for 2 days. Xylem sap samples were collected as described previously (Ma *et al*, 2004). Xylem sap samples were diluted in 5% $HNO_3$ and $Na^+$ contents of the samples were measured by ICP-OES.

### *Transient gene expression analyses*

The EGFP DNA fragment was amplified by PCR and subcloned into the pBI221 vector (Clontech, Mountain View, CA, USA). The coding region of the *OsHKT2;1* cDNA was also amplified and fused in frame to the 3′ end of the EGFP DNA. EGFP-OsHKT2;1 and control constructs were introduced into protoplasts of leaf mesophyll cells of tobacco (*Nicotiana tabacum*) cv. SR1 by polyethylene–glycol-mediated transformation, as described previously (Sparla *et al*, 2006). Before confocal microscopy, FM4-64 (Invitrogen Molecular probes, Eugene, OR, USA) was added to protoplast incubation solutions at a final concentration of 17 μM and incubated for 2 min at room temperature. Fluorescence was analyzed by confocal microscopy (Eclipse TE2000-U; Nikon, Tokyo, Japan), using 488 nm excitation and either 510 nm emission filters for EGFP or 600 nm emission filters for FM4-64.

EGFP-OsHKT2;1 and control constructs were also introduced into leaf epidermal cells of *Arabidopsis* (Columbia). Abaxial sides of WT plants grown on soil for 20 days were transfected by bombardment (PDS-000/He; Bio-Rad, Hercules, CA, USA) (Arnim *et al*, 1998). After 1 day, GFP expression was examined by confocal microscopy (Eclipse TE2000-U, Nikon, Tokyo, Japan).

### *Tracer influx analyses*

Rice plants were grown in 1 mM $CaSO_4$ solution or the same solution supplemented with the indicated concentrations of KCl or NaCl. Influx assays were performed as described previously (Gierth *et al*, 2005), with minor modifications described below. The influx buffer was composed of 2 mM MES-1,3 bis[tris(hydroxymethyl9-methylamino)]propane (BTP) pH5.5, 1 mM $CaCl_2$ supplemented with either cold NaCl and $^{22}$NaCl (Amersham Bioscience, Pittsburgh, PA, USA) in $Na^+$ influx assays or RbCl and $^{86}$RbCl (Amersham Bioscience, Pittsburgh, PA, USA) in $Rb^+$ uptake assays. The same solution, excluding radioisotope, was used as a washing buffer. $K^+$-starved intact plants were pretreated with the indicated concentrations of each inhibitor in the presence of 1 mM $CaSO_4$ for 1 h. Plants were incubated for 20 min except for time-dependent influx assays. Excised roots were placed into a liquid scintillation vial and radioactivity was measured with a scintillation counter (LS6500 Beckman, Fullerton, CA, USA).

### *Supplementary data*

Supplementary data are available at *The EMBO Journal* Online (http://www.embojournal.org).

## Acknowledgements

We thank Drs Markus Gierth (University of Cologne, Germany) and Mamoru Okamoto (University of California, San Diego) for helpful discussions regarding tracer influx experiments and quantitative real-time RT–PCR analyses. This work was supported by grants from the US Department of Energy (DOE-DE-FG02-03ER15449), the National Institutes of Health (ES010337-GM060396) and the National Science Foundation (MCB0417118) to JIS and the Crop Functional Genomic Center of the 21st Century Frontier Program (Grant CG1111) to GA.

 

## References


Aharon GS, Apse MP, Duan S, Hua X, Blumwald E (2003) Characterization of a family of vacuolar $Na^+/H^+$ antiporters in *Arabidopsis thaliana*. *Plant Soil* **253:** 245–256

Amtmann A, Laurie S, Leigh R, Sanders D (1997) Multiple inward channels provide flexibility in $K^+/Na^+$ discrimination at the plasma membrane of barley suspension culture cells. *J Exp Bot* **48:** 431–440

Apse MP, Aharon GS, Snedden WA, Blumwald E (1999) Salt tolerance conferred by overexpression of a vacuolar $Na^+/H^+$ antiport in *Arabidopsis*. *Science* **285:** 1256–1258

Apse MP, Sottosanto JB, Blumwald E (2003) Vacuolar cation/$H^+$ exchange, ion homeostasis, and leaf development are altered in a T-DNA insertional mutant of *AtNHX1*, the *Arabidopsis* vacuolar $Na^+/H^+$ antiporter. *Plant J* **36:** 229–239

Arnim AG, Deng XW, Stacey MG (1998) Cloning vectors for the expression of green fluorescent protein fusion proteins in transgenic plants. *Gene* **221:** 35–43

Berthomieu P, Conejero G, Nublat A, Brackenbury WJ, Lambert C, Savio C, Uozumi N, Oiki S, Yamada K, Cellier F, Gosti F, Simonneau T, Essah PA, Tester M, Very AA, Sentenac H, Casse F (2003) Functional analysis of *AtHKT1* in *Arabidopsis* shows that $Na^+$ recirculation by the phloem is crucial for salt tolerance. *EMBO J* **22:** 2004–2014

Besford RT (1978) Effect of replacing nutrient potassium by sodium in uptake and distribution of sodium in tomato plants. *Plant Soil* **50:** 399–409

Blumwald E, Poole R (1985) $Na^+/H^+$-antiport in isolated tonoplast vesicles from storage tissue of *Beta vulgaris*. *Plant Physiol* **78:** 163–167

Blumwald E, Poole RJ (1987) Salt tolerance in suspension cultures of sugar beet: induction of $Na^+/H^+$ antiport activity at the tonoplast by growth in salt. *Plant Physiol* **83:** 884–887

Bolte S, Talbot C, Boutte Y, Catrice O, Read ND, Satiat-Jeunemaitre B (2004) FM-dyes as experimental probes for dissecting vesicle trafficking in living plant cells. *J Microsc* **214:** 159–173

Buschmann PH, Vaidyanathan R, Gassmann W, Schroeder JI (2000) Enhancement of $Na^+$ uptake currents, time-dependent inward-rectifying $K^+$ channel currents, and $K^+$ channel transcripts by $K^+$ starvation in wheat root cells. *Plant Physiol* **122:** 1387–1397

Byrt CS, Platten JD, Spielmeyer W, James RA, Lagudah ES, Dennis ES, Tester M, Munns R (2007) HKT1;5-like cation transporters linked to $Na^+$ exclusion loci in wheat, *Nax2* and *Kna1*. *Plant Physiol* **143:** 1918–1928

Davenport RJ, Tester M (2000) A weakly voltage-dependent, non-selective cation channel mediates toxic sodium influx in wheat. *Plant Physiol* **122:** 823–834

Essah PA, Davenport R, Tester M (2003) Sodium influx and accumulation in *Arabidopsis*. *Plant Physiol* **133:** 307–318

Fairbairn DJ, Liu W, Schachtman DP, Gomez-Gallego S, Day SR, Teasdale RD (2000) Characterisation of two distinct HKT1-like potassium transporters from *Eucalyptus camaldulensis*. *Plant Mol Biol* **43:** 515–525

Flowers TJ, Läuchli A (1983) Sodium versus potassium: substitution and compartmentation. *Inorganic Plant Nutrition* **15b:** 651–681

Garciadeblás B, Senn ME, Bañuelos MA, Rodríguez-Navarro A (2003) Sodium transport and HKT transporters: the rice model. *Plant J* **34:** 788–801

Gassmann W, Rubio F, Schroeder JI (1996) Alkali cation selectivity of the wheat root high-affinity potassium transporter HKT1. *Plant J* **10:** 852–869

Gaxiola RA, Rao R, Sherman A, Grisafi P, Alper SL, Fink GR (1999) The *Arabidopsis thaliana* proton transporters, AtNhx1 and Avp1, can function in cation detoxification in yeast. *Proc Natl Acad Sci USA* **96:** 1480–1485

Gierth M, Mäser P, Schroeder JI (2005) The potassium transporter AtHAK5 functions in $K^+$ deprivation-induced high-affinity $K^+$ uptake and AKT1 $K^+$ channel contribution to $K^+$ uptake kinetics in *Arabidopsis* roots. *Plant Physiol* **137:** 1105–1114

Glenn E, Brown J, Blumwald E (1999) Salt tolerance and crop potential of halophytes. *Crit Rev Plant Sci* **18:** 227–256

Gobert A, Park G, Amtmann A, Sanders D, Maathuis FJ (2006) *Arabidopsis thaliana* cyclic nucleotide gated channel 3 forms a non-selective ion transporter involved in germination and cation transport. *J Exp Bot* **57:** 791–800

Golldack D, Su H, Quigley F, Kamasani UR, Munoz-Garay C, Balderas E, Popova OV, Bennett J, Bohnert HJ, Pantoja O (2002) Characterization of a HKT-type transporter in rice as a general alkali cation transporter. *Plant J* **31:** 529–542

Gong JM, Waner DA, Horie T, Li SL, Horie R, Abid KB, Schroeder JI (2004) Microarray-based rapid cloning of an ion accumulation deletion mutant in *Arabidopsis thaliana*. *Proc Natl Acad Sci USA* **101:** 15404–15409

Haro R, Bañuelos MA, Senn ME, Barrero-Gil J, Rodríguez-Navarro A (2005) HKT1 mediates sodium uniport in roots. Pitfalls in the expression of HKT1 in yeast. *Plant Physiol* **139:** 1495–1506

Hirochika H (1997) Retrotransposons of rice: their regulation and use for genome analysis. *Plant Mol Biol* **35:** 231–240

Hirochika H (2001) Contribution of the *Tos17* retrotransposon to rice functional genomics. *Curr Opin Plant Biol* **4:** 118–122

Horie T, Horie R, Chan WY, Leung HY, Schroeder JI (2006) Calcium regulation of sodium hypersensitivities of *sos3* and *athkt1* mutants. *Plant Cell Physiol* **47:** 622–633

Horie T, Schroeder JI (2004) Sodium transporters in plants. Diverse genes and physiological functions. *Plant Physiol* **136:** 2457–2462

Horie T, Yoshida K, Nakayama H, Yamada K, Oiki S, Shinmyo A (2001) Two types of HKT transporters with different properties of $Na^+$ and $K^+$ transport in *Oryza sativa*. *Plant J* **27:** 129–138

Huang S, Spielmeyer W, Lagudah ES, James RA, Platten JD, Dennis ES, Munns R (2006) A sodium transporter (HKT7) is a candidate for *Nax1*, a gene for salt tolerance in durum wheat. *Plant Physiol* **142:** 1718–1727

Laurie S, Feeney KA, Maathuis FJ, Heard PJ, Brown SJ, Leigh RA (2002) A role for HKT1 in sodium uptake by wheat roots. *Plant J* **32:** 139–149

Ma JF, Mitani N, Nagao S, Konishi S, Tamai K, Iwashita T, Yano M (2004) Characterization of the silicon uptake system and molecular mapping of the silicon transporter gene in rice. *Plant Physiol* **136:** 3284–3289

Maathuis FJ, Sanders D (2001) Sodium uptake in *Arabidopsis* roots is regulated by cyclic nucleotides. *Plant Physiol* **127:** 1617–1625

Marschner H (1971) Why can sodium replace potassium in plants?. Proceedings of the 8th Colloquium of the International Potash Institute, Uppsala, Sweden, 1971. Int. Potash Institute: Berne

Mäser P, Eckelman B, Vaidyanathan R, Horie T, Fairbairn DJ, Kubo M, Yamagami M, Yamaguchi K, Nishimura M, Uozumi N, Robertson W, Sussman MR, Schroeder JI (2002a) Altered shoot/root $Na^+$ distribution and bifurcating salt sensitivity in *Arabidopsis* by genetic disruption of the $Na^+$ transporter AtHKT1. *FEBS Lett* **531:** 157–161

Mäser P, Hosoo Y, Goshima S, Horie T, Eckelman B, Yamada K, Yoshida K, Bakker EP, Shinmyo A, Oiki S, Schroeder JI, Uozumi N (2002b) Glycine residues in potassium channel-like selectivity filters determine potassium selectivity in four-loop-per-subunit HKT transporters from plants. *Proc Natl Acad Sci USA* **99:** 6428–6433

Mengel K, Kirkby EA (1982) *Principles of Plant Nutrition, 3rd edn*. Worblaufen-Bern, Switzerland: International Potash Institute pp 425–426

Miyao A, Tanaka K, Murata K, Sawaki H, Takeda S, Abe K, Shinozuka Y, Onosato K, Hirochika H (2003) Target site specificity of the *Tos17* retrotransposon shows a preference for insertion within genes and against insertion in retrotransposon-rich regions of the genome. *Plant Cell* **15:** 1771–1780

Murashige T, Skoog F (1962) A revised medium for rapid growth and bioassays in tobacco tissue cultures. *Physiol Plant* **15:** 473–497

Murguía JR, Bellés JM, Serrano R (1995) A salt-sensitive 3′(2′), 5′-bisphosphate nucleotidase involved in sulfate activation. *Science* **267:** 232–234

Platten JD, Cotsaftis O, Berthomieu P, Bohnert H, Davenport RJ, Fairbairn DJ, Horie T, Leigh RA, Lin HX, Luan S, Maser P, Pantoja O, Rodriguez-Navarro A, Schachtman DP, Schroeder JI, Sentenac H, Uozumi N, Very AA, Zhu JK, Dennis ES, Tester M (2006) Nomenclature for HKT transporters, key determinants of plant salinity tolerance. *Trends Plant Sci* **11:** 372–374

Rains DW, Epstein E (1965) Transport of sodium in plant tissue. *Science* **148:** 1611

Rains DW, Epstein E (1967a) Sodium absorption by barley roots: role of the dual mechanisms of alkali cation transport. *Plant Physiol* **42:** 314–318

Rains DW, Epstein E (1967b) Sodium absorption by barley roots: its mediation by mechanism 2 of alkali cation transport. *Plant Physiol* **42:** 319–323

Ren ZH, Gao JP, Li LG, Cai XL, Huang W, Chao DY, Zhu MZ, Wang ZY, Luan S, Lin HX (2005) A rice quantitative trait locus for salt tolerance encodes a sodium transporter. *Nat Genet* **37:** 1141–1146

Roberts S, Tester M (1997) A patch clamp study of $Na^+$ transport in maize roots. *J Exp Bot* **48:** 431–440

Rubio F, Gassmann W, Schroeder JI (1995) Sodium-driven potassium uptake by the plant potassium transporter HKT1 and mutations conferring salt tolerance. *Science* **270:** 1660–1663

Rus A, Yokoi S, Sharkhuu A, Reddy M, Lee BH, Matsumoto TK, Koiwa H, Zhu JK, Bressan RA, Hasegawa PM (2001) AtHKT1 is a salt tolerance determinant that controls $Na^+$ entry into plant roots. *Proc Natl Acad Sci USA* **98:** 14150–14155

Schachtman DP, Schroeder JI (1994) Structure and transport mechanism of a high-affinity potassium uptake transporter from higher plants. *Nature* **370:** 655–658

Schroeder JI, Ward JM, Gassmann W (1994) Perspectives on the physiology and structure of inward-rectifying $K^+$ channels in higher plants: biophysical implications for $K^+$ uptake. *Annu Rev Biophys Biomol Struct* **23:** 441–471

Shi H, Ishitani M, Kim C, Zhu JK (2000) The *Arabidopsis thaliana* salt tolerance gene *SOS1* encodes a putative $Na^+/H^+$ antiporter. *Proc Natl Acad Sci USA* **97:** 6896–6901

Shi H, Quintero FJ, Pardo JM, Zhu JK (2002) The putative plasma membrane $Na^+/H^+$ antiporter SOS1 controls long-distance $Na^+$ transport in plants. *Plant Cell* **14:** 465–477

Sparla F, Costa A, Lo Schiavo F, Pupillo P, Trost P (2006) Redox regulation of a novel plastid-targeted beta-amylase of *Arabidopsis*. *Plant Physiol* **141:** 840–850

Su H, Balderas E, Vera-Estrella R, Golldack D, Quigley F, Zhao C, Pantoja O, Bohnert HJ (2003) Expression of the cation transporter McHKT1 in a halophyte. *Plant Mol Biol* **52:** 967–980

Sunarpi, Horie T, Motoda J, Kubo M, Yang H, Yoda K, Horie R, Chan WY, Leung HY, Hattori K, Konomi M, Osumi M, Yamagami M, Schroeder JI, Uozumi N (2005) Enhanced salt tolerance mediated by AtHKT1 transporter-induced $Na^+$ unloading from xylem vessels to xylem parenchyma cells. *Plant J* **44:** 928–938

Swarup R, Kargul J, Marchant A, Zadik D, Rahman A, Mills R, Yemm A, May S, Williams L, Millner P, Tsurumi S, Moore I, Napier R, Kerr ID, Bennett MJ (2004) Structure–function analysis of the presumptive *Arabidopsis* auxin permease AUX1. *Plant Cell* **16:** 3069–3083

Tholema N, Vor der Bruggen M, Maser P, Nakamura T, Schroeder JI, Kobayashi H, Uozumi N, Bakker EP (2005) All four putative selectivity filter glycine residues in KtrB are essential for high affinity and selective $K^+$ uptake by the KtrAB system from *Vibrio alginolyticus*. *J Biol Chem* **280:** 41146–41154

Tsugane K, Kobayashi K, Niwa Y, Ohba Y, Wada K, Kobayashi H (1999) A recessive *Arabidopsis* mutant that grows photoautotrophically under salt stress shows enhanced active oxygen detoxification. *Plant Cell* **11:** 1195–1206

Tyerman S, Skerrett M, Garrill A, Findlay G, Leigh R (1997) Pathways for the permeation of $Na^+$ and $Cl^-$ into protoplasts derived from the cortex of wheat roots. *J Exp Bot* **48:** 459–480

Uozumi N, Kim EJ, Rubio F, Yamaguchi T, Muto S, Tsuboi A, Bakker EP, Nakamura T, Schroeder JI (2000) The *Arabidopsis HKT1* gene homolog mediates inward $Na^+$ currents in *Xenopus laevis* oocytes and $Na^+$ uptake in *Saccharomyces cerevisiae*. *Plant Physiol* **122:** 1249–1259

Ward JM, Hirschi KD, Sze H (2003) Plants pass the salt. *Trends Plant Sci* **8:** 200–201

Woolley TJ (1957) Sodium and silicon as nutrient for the tomato plant. *Plant Physiol* **32:** 317–321

Wu SJ, Ding L, Zhu JK (1996) *SOS1*, a genetic locus essential for salt tolerance and potassium acquisition. *Plant Cell* **8:** 617–627

Yamazaki M, Tsugawa H, Miyao A, Yano M, Wu J, Yamamoto S, Matsumoto T, Sasaki T, Hirochika H (2001) The rice retrotransposon *Tos17* prefers low-copy-number sequences as integration targets. *Mol Genet Genomics* **265:** 336–344

Yeo AR, Yeo ME, Flowers TJ (1987) The contribution of an apoplastic pathway to sodium uptake by rice roots in saline conditions. *J Exp Bot* **38:** 1141–1153

Yokoi S, Quintero FJ, Cubero B, Ruiz MT, Bressan RA, Hasegawa PM, Pardo JM (2002) Differential expression and function of *Arabidopsis thaliana NHX* $Na^+/H^+$ antiporters in the salt stress response. *Plant J* **30:** 529–539

Zhu JK (2002) Salt and drought stress signal transduction in plants. *Annu Rev Plant Biol* **53:** 247–273

 